APPLYING AN HP-ADAPTIVE DISCONTINUOUS GALERKIN SCHEME TO BEAM DYNAMICS SIMULATIONS*

S. Schnepp†, Graduate School of Computational Engineering, TU Darmstadt, Germany
E. Gjonaj‡, T. Weiland§, Institut für Theorie Elektromagnetischer Felder, TU Darmstadt, Germany

Abstract

An adaptive high order discontinuous Galerkin (DG) scheme for performing beam dynamics simulations is presented. We elaborate on h- and p-adaptations, the former modifying the actual size of computational elements and the latter the dimension of the associated approximation space. The efficiency and stability of the adaptation techniques are emphasized. The scheme is applied in order to perform hp-adaptive beam dynamics simulations. We compare the results with the analytical solution and demonstrate that the adaptive scheme requires significantly less computational resources for obtaining a certain accuracy.

INTRODUCTION

The problem of self-consistent simulations of short relativistic particle bunches in long accelerator structures exhibits a pronounced multi-scale character. The adequate resolution of the THz space charge fields excited by short ultra-relativistic bunches requires mesh spacings in the micrometer range. On the other hand, the discretization of complete accelerator sections using such fine meshes results in a prohibitive number of Degrees of Freedom (DoF). Due to the spatial concentration of the particles and the excited space charge fields, the application of time-adaptive mesh refinement is an emerging idea. We reported on the implementation of time-adaptive mesh refinement for the Finite Integration Technique (FIT) [1]. Based on this work, an adaptive discontinuous Galerkin (DG) code was implemented. Within the DG method, the electromagnetic field solution is approximated elementwise, employing a set of basis functions. This provides two options for adapting the local accuracy of the DG approximation. First, the size of the grid elements can be varied. This is referred to as h-adaptation. Additionally, the maximum order of the employed basis functions can be modified, which is referred to as p-adaptation. Combining both options yields an hp-adaptive method. The twofold refinement mechanisms of the hp-adaptive DG method offer maximum freedom for the approximation of the electromagnetic field solution.

* The work of S. Schnepp is supported by the 'Initiative for Excellence' of the German Federal and State Governments and the Graduate School of Computational Engineering at Technische Universität Darmstadt.

† schnepp@gsc.tu-darmstadt.de
‡ gjonaj@temf.tu-darmstadt.de
§ weiland@temf.tu-darmstadt.de

DISCONTINUOUS GALERKIN METHOD FOR MAXWELL'S EQUATIONS

Spatial Discretization Procedure

Given a decomposition of the computational domain Ω into N non-overlapping, hexahedral elements $\{C_i\}$, $i = 1..N$, a set of linearly independent basis functions $\{\varphi_i^p\}$, $p = 0..P$ for every cell is defined, where P denotes the highest order employed. The basis functions are required to be continuous within the cell C_i and vanish otherwise

$$\varphi_i^p(\mathbf{r}) = \begin{cases} \varphi^p(\mathbf{r}), & \mathbf{r} \in C_i, \\ 0, & \text{otherwise.} \end{cases} \quad (1)$$

Subsequently, the space and time continuous electromagnetic field quantities **E** and **H** are approximated in the form

$$\mathbf{E}(\mathbf{r},t) \approx \widetilde{\mathbf{E}}(\mathbf{r},t) = \sum_i \widetilde{\mathbf{E}}_i(\mathbf{r},t) = \sum_{i,p} e_i^p(t)\varphi_i^p(\mathbf{r}), \quad (2)$$

$$\mathbf{H}(\mathbf{r},t) \approx \widetilde{\mathbf{H}}(\mathbf{r},t) = \sum_i \widetilde{\mathbf{H}}_i(\mathbf{r},t) = \sum_{i,p} h_i^p(t)\varphi_i^p(\mathbf{r}), \quad (3)$$

where $\widetilde{\mathbf{E}}$ and $\widetilde{\mathbf{H}}$ denote the approximate field vectors. The numerical DoF are denoted by e_i^p and h_i^p. They are gathered in the vectors **e** and **h**.

Substituting the electromagnetic quantities by their approximations in Faraday's and Ampère's law and applying the Galerkin procedure yields the weak DG formulation [2]. Due to the cell-wise compact support of the basis functions (1), the approximations (2) and (3) will, in general, be discontinuous at element interfaces. Continuity is enforced only in the weak sense via numerical fluxes. Among the different flux definitions, we chose centered fluxes. As demonstrated in [2, 3] this ensures the strict conservation of the electromagnetic energy. Using the naming convention given there and vector notation for all terms, the semidiscrete formulation reads

$$\frac{\mathrm{d}}{\mathrm{d}t}\begin{pmatrix}\mathbf{M}_\epsilon\mathbf{e}\\ \mathbf{M}_\mu\mathbf{h}\end{pmatrix} + \begin{pmatrix}\mathbf{0} & -\mathbf{C}\\ \mathbf{C}^{\mathrm{T}} & \mathbf{0}\end{pmatrix}\begin{pmatrix}\mathbf{e}\\ \mathbf{h}\end{pmatrix} = -\begin{pmatrix}\mathbf{j}\\ \mathbf{0}\end{pmatrix}. \quad (4)$$

The terms $\mathbf{M}_\epsilon$ and $\mathbf{M}_\mu$ are the mass matrices and $\mathbf{C}$ denotes the weak DG curl operator. The vector $\mathbf{j}$ represents the convective currents.

In the particular case of particle accelerator problems, the issue of charge conservation is specially relevant due to the existence of freely moving charges. In [3] it was shown that strict charge conservation is guaranteed if, and only if, a tensor product basis on conforming Cartesian grids is

applied for the approximations (2) and (3). The continuous current density is given by

$$\mathbf{J}(\mathbf{r},t) = \sum_{k=1}^{N_p} Q_k \mathbf{v}_k S(|\mathbf{r}_k - \mathbf{r}|), \tag{5}$$

where Q_k is the charge carried by the k-th of N_p particles, $\mathbf{r}_k$ and $\mathbf{v}_k$ are its position and velocity vector and S is a distribution function describing the assumed particle shape. In case S corresponds to the Kronecker delta, the particles are modeled as point charges. Other shape functions are discussed in [4]. Integrating the current density over one time step and projecting to the basis functions yields the DG approximation

$$(j_i^p)^n = \frac{\left(\varphi_i^p, \int_{(n-1)\Delta t}^{n\Delta t} \mathbf{J}(\mathbf{r},t)\mathrm{d}t\right)_{C_i}}{(\varphi_i^p, \varphi_i^p)_{C_i}}. \tag{6}$$

Above, $(a,b)_{C_i}$ denotes the inner product of a and b on C_i, Δt is the time step and n the time step number.

Suitability for hp-Adaptation

The discontinuous Galerkin method is highly suited for the application of h- and p-adaptation techniques. Independently of the approximation order, the method always preserve the same high degree of locality. Due to the element-wise compact support, individual elements communicate only via interface fluxes. The computation of these, in turn, involves only the interface values of direct neighbors. Splitting and merging of elements, hence, is a purely local operation, which affects none but the adapted elements. For our particular setup of Cartesian grids and a tensor product basis, this adaptation can be performed very efficiently, as it will be shown in the following section. Since additionally, assigning different approximation orders throughout the elements of the computational domain is readily possible, the method is well-suited for an *hp*-adaptive procedure, i.e., adapting the local grid step size, as well as the local approximation order in a problem oriented fashion.

ADAPTATION TECHNIQUES

h-Adaptation

When performing *h*-adaptation the size of dedicated elements is modified locally by splitting them into subelements or, conversely, by merging them into larger ones. The grid topology is, thus, altered while the approximation orders of the involved elements are kept constant.

In the case of h-refinement, the approximations within the subelements are obtained by projecting the existing approximation onto the support of the subelements. We restrict ourselves to the bisection of elements and do not consider other division ratios. Continuous basis functions $\psi_{i,\mathrm{l}}$ and $\psi_{i,\mathrm{r}}$ are defined within the interior of the left and right

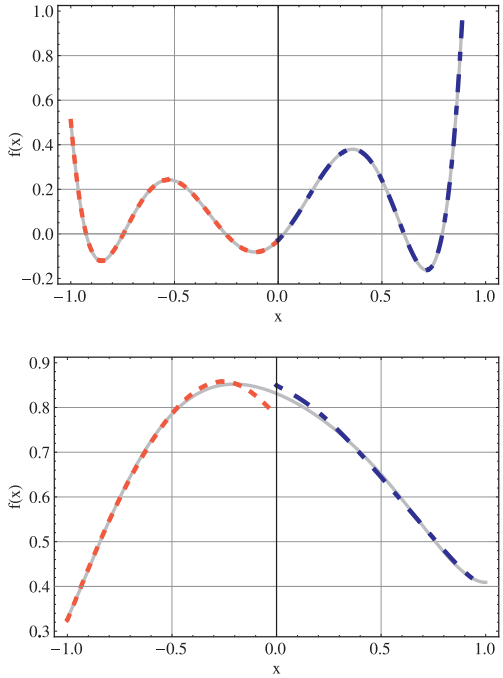

Figure 1: For the splitting of elements (top), the approximate solution within the element C_i (gray, solid) is accurately projected onto its subelements $C_{i,\mathrm{l}}$ (red, dotted) and $C_{i,\mathrm{r}}$ (blue, dash-dotted). Due to the discontinuity the approximation within the merged element cannot be exact (bottom).

subelement $C_{i,\mathrm{l}}$ and $C_{i,\mathrm{r}}$ and set identically zero elsewhere. The integral terms

$$\mathbf{P}_{\mathrm{l}}^{qp} = \frac{(\varphi^p,\, \psi_{\mathrm{l}}^q)_{C_{i,\mathrm{l}}}}{(\psi_{\mathrm{l}}^q,\, \psi_{\mathrm{l}}^q)_{C_{i,\mathrm{l}}}} \quad \text{and} \quad \mathbf{P}_{\mathrm{r}}^{qp} = \frac{(\varphi^p,\, \psi_{\mathrm{r}}^q)_{C_{i,\mathrm{r}}}}{(\psi_{\mathrm{r}}^q,\, \psi_{\mathrm{r}}^q)_{C_{i,\mathrm{r}}}}, \tag{7}$$

for $p,q = 1..P$ determine the entries of the projection matrices $\mathbf{P}_{\mathrm{l}}$ and $\mathbf{P}_{\mathrm{r}}$. Each term describes the contribution of the basis function of order p of the element C_i to the basis function of order q of its subelements. The numerical DoF of the subelements, $\mathbf{e}_{i,\mathrm{l}}$, $\mathbf{e}_{i,\mathrm{r}}$ and $\mathbf{h}_{i,\mathrm{l}}$, $\mathbf{h}_{i,\mathrm{r}}$, are obtained by means of the matrix-vector multiplications

$$\mathbf{e}_{i,\mathrm{l}} = \mathbf{P}_{\mathrm{l}}\mathbf{e}_i, \qquad \mathbf{e}_{i,\mathrm{r}} = \mathbf{P}_{\mathrm{r}}\mathbf{e}_i, \tag{8}$$

$$\mathbf{h}_{i,\mathrm{l}} = \mathbf{P}_{\mathrm{l}}\mathbf{h}_i, \qquad \mathbf{h}_{i,\mathrm{r}} = \mathbf{P}_{\mathrm{r}}\mathbf{h}_i. \tag{9}$$

These operations are exact in the sense that the approximation within the subelements is identical to the approximation within the original element in every point. This is shown in Figure 1 (top).

For the converse process, i.e., merging of elements, it is not possible to obtain an exact representation within the merged element due to the discontinuous character of the approximations. The approximation within C_i is considered to be given piecewise on the subelements with the DoF $\mathbf{e}_{i,\mathrm{l}}$, $\mathbf{e}_{i,\mathrm{r}}$ and $\mathbf{h}_{i,\mathrm{l}}$, $\mathbf{h}_{i,\mathrm{r}}$. The entries of the projection matrix

$\mathbf{P}_{\mathrm{m}}$ are specified by

$$\mathbf{P}_{\mathrm{m}}^{qp} = \frac{(\psi_{\mathrm{l}}^q + \psi_{\mathrm{r}}^q,\, \varphi^p)_{C_i}}{(\varphi^p,\, \varphi^p)_{C_i}} = \frac{(\psi_{\mathrm{l}}^q,\, \varphi^p)_{C_i}}{(\varphi^p,\, \varphi^p)_{C_i}} + \frac{(\psi_{\mathrm{r}}^q,\, \varphi^p)_{C_i}}{(\varphi^p,\, \varphi^p)_{C_i}} = \mathbf{P}_{\mathrm{m,l}}^{qp} + \mathbf{P}_{\mathrm{m,r}}^{qp}. \tag{10}$$

Summing up the contributions of the subelements yields the DoF of the merged element

$$\mathbf{e}_i = \mathbf{P}_{\mathrm{m,l}}\mathbf{e}_{i,\mathrm{l}} + \mathbf{P}_{\mathrm{m,r}}\mathbf{e}_{i,\mathrm{r}}, \tag{11}$$

$$\mathbf{h}_i = \mathbf{P}_{\mathrm{m,l}}\mathbf{h}_{i,\mathrm{l}} + \mathbf{P}_{\mathrm{m,r}}\mathbf{h}_{i,\mathrm{r}}. \tag{12}$$

The matrices $\mathbf{P}_{\mathrm{m,l}}$ and $\mathbf{P}_{\mathrm{m,r}}$, as well as $\mathbf{P}_{\mathrm{l}}$ and $\mathbf{P}_{\mathrm{r}}$, do not depend upon the actual approximation but only on the basis functions. They can be evaluated analytically and stored for repeated use.

p-Adaptation

P-adaptation refers to a local or global modification of the approximation order P while keeping the mesh unaltered. In time-domain simulations *p*-adaptation can be efficiently implemented if a set of hierarchical basis functions is employed. In this case, the DoF associated with the different approximation orders do not depend upon each other. Thus, increasing the approximation order is as simple as preserving the current coefficients and attaching those of the next higher order basis functions to the DoF vectors $\mathbf{e}_i$ and $\mathbf{h}_i$ for the respective element C_i. The new coefficients are initialized to zero. In order to reduce the order, the DoF associated with the higher order basis functions are dismissed.

hp-Adaptation

For smooth solutions, the approximation order is directly linked to the asymptotic convergence order. It is, thus, desirable to work with high order elements. However, the convergence order breaks down if the solution is non-smooth. In Fig. 2 the error of the DG approximation to a Gaussian and a trapezoidal field distribution is shown. The error is plotted versus the grid step size, both of them on a logarithmic scale. The approximation error of the Gaussian (top) reduces with the expected rate for increased P. For the trapezoidal distribution (bottom), however, the convergence rate stagnates for higher approximation orders. An important key point of an hp-adaptation algorithm is, hence, the detection of regions with a low degree of solution smoothness. Also, regions of low electromagnetic field energy should be identified since they probably do not require a high resolution.

Efficiency and Stability

We employ the orthogonal set of Legendre polynomials as basis functions and define a tensor product basis for conforming Cartesian grids. This particular setting allows for a very efficient implementation of the DG method since all inner products of basis and test functions reduce to zero if their order differs and to a factor which depends only on the dimensions of the respective element, otherwise.

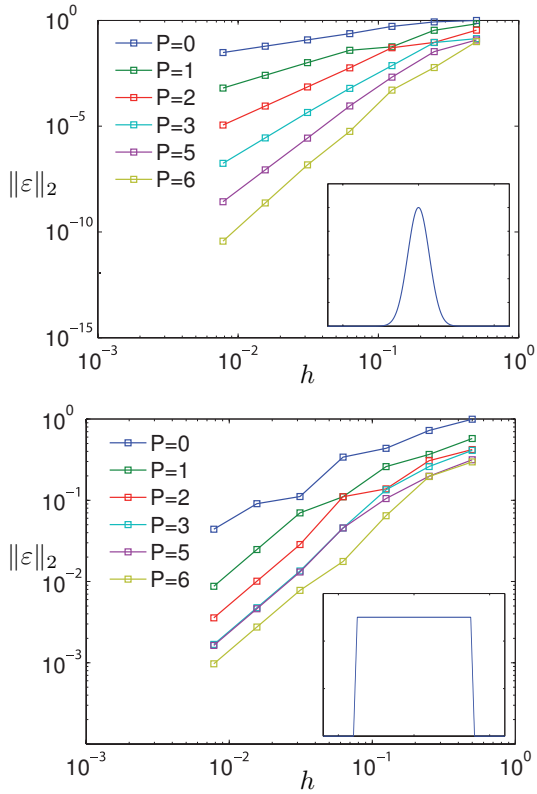

Figure 2: Approximation error in the L^2-norm of a Gaussian (top) and a trapezoidal distribution (bottom) versus the grid step. For the smooth function in the top graph the expected convergence rate is observed. For the non-smooth function in the bottom graph the convergence rate breaks down.

The projection based h-adaptation can also be implemented in a very efficient manner since the projection matrices do not vary with time. They have to be evaluated only once, which can be done analytically. During the actual simulation, we additionally benefit from the Cartesian grids and the tensor product basis ansatz since the bisection of elements and the calculation of the coefficients within the modified elements can also be performed very efficiently.

It remains to address the stability of the adaptation techniques. The adaptations are stable if their application does not increase the electromagnetic energy within the modified elements. The energy of the element C_i reads

$$W_i = \frac{1}{2}|C_i|\left(\epsilon_i\|\mathbf{e}_i\|_2^2 + \mu_i\|\mathbf{h}_i\|_2^2\right), \tag{13}$$

where $|C_i|$ denotes the volume of C_i and ϵ_i, μ_i are its permittivity and permeability.

It is readily seen that a p-reduction induces a loss of the discrete energy associated with the respective coefficients.

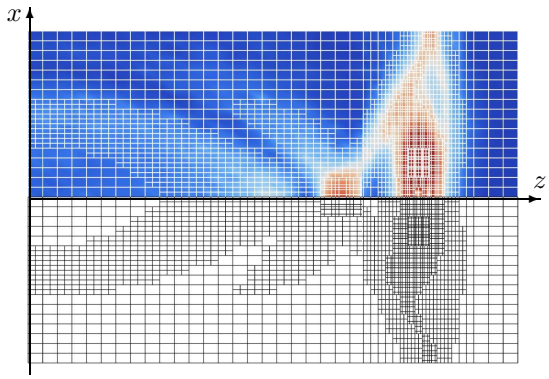

Figure 3: Snapshot of the total electric field excited by a bunch of particles in cut view. The upper half shows the electric field and the computational grid, the lower half shows the hp-adapted grid exclusively.

The coefficients, which are added during p-enrichment are initialized by zero. In this case W_i is preserved.

We will not present formal derivations of the stability of the h-adaptations but rather state their results. Details are found in [5]. In the case of h-refinement, the sum of the discrete energies of the subelements is equal to the energy of the parent element. Since the approximations within the subelements exactly represent the original approximation this is consequential. For h-coarsening the energy is at most preserved. The application of p-enrichment or h-refinement, hence, conserves the discrete energy exactly while p-reduction or h-coarsening usually induce a loss of energy.

APPLICATIONS

The method has been applied to the simulation of a particle bunch drifting with the constant velocity $v = 0.9c_0$ in a cylindrical perfectly electrically conducting tube, where c_0 is the speed of light in vacuum. The electromagnetic field solution for this situation at an arbitrary point in time is described in [6], where the tube is considered semi-infinite in the direction of bunch propagation. The length and radius of the tube are set to 120 mm and 40 mm respectively. The particle distribution of the bunch is Gaussian with an RMS length and radius of 5 mm and 3 mm, respectively.

We apply hp-adaptation for the simulation of the problem. The p-adaptation is controlled by the field amplitude. In addition, h-refinement is applied to the elements containing particles and all neighboring elements with the same index along the z-axis. This ensures a conforming grid refinement. Fig. 3 shows the total electric field along with the hp-adapted grid. For the p-adaptation a range of one through four for the approximation orders was applied. In order to visualize the approximation order of an element, the respective number of collocation points are plotted. Along the z-direction an additional conforming h-refinement is applied to the elements, which contain particles and all neighboring elements with the same z-index.

Table 1: Relative error and total variation of solutions obtained by the non-adaptive and adaptive scheme using various settings.

L	P_{min}	P_{max}	≈DoF / 1e6	Time / sec	ε^{rel}	TV
0	1	1	6.80	310	0.081	8.71
0	2	2	22.96	2020	0.042	4.15
1	1	3	9.00	1170	0.043	2.68
1	1	4	10.50	1650	0.028	1.00

The relative L^∞-error and the total variation (TV) [7] of the electric field along the cylinder axis are given as measures for the quality of the numerical solutions. The TV is a measure for the smoothness of a function. It is defined as

$$TV(\mathbf{E}(z)) = \int |\mathbf{E}'(z)| \mathrm{d}z. \tag{14}$$

Table 1 summarizes the results. The number of h-refinement levels is denoted by L. The grid step sizes and the h-refinement level are chosen such that the minimum step size remains identical. The total variation is normalized to the smallest value obtained. The adaptive simulations consume more time per DoF. Partly, the extra time is spent for the adaptation routines, and partly it is due to the reduced maximally stable time step connected with higher approximation orders.

As a second application, we have simulated a part of the PITZ injector (Photo Injector Test Facility at DESY Zeuthen) [8]. The PITZ project was initiated in order to test and optimize sources of high brightness electron beams for future free electron lasers (FELs) and linear colliders. Fig. 4 shows the total electric field and hp-adapted grid in a y-cut through the three-dimensional domain. The simulated section consists of the 1.5 cell RF gun and has a length of 25 cm. This grid was generated for illustration purposes only. Accurate simulations require a higher resolution. Nevertheless, it demonstrates the ability of the scheme to handle more complex situations.

OUTLOOK ON ERROR BASED AUTOMATIC HP-ADAPTATION

For the examples presented above, we used a naive algorithm for controlling the hp-adaptation. The approximation order p of every element, e.g., is determined from a comparison of its field magnitude with the maximum field magnitude. However, the adaptation should be based on the approximation error, which is for general examples not linked to the field magnitude. In [9] it is shown that the residual relates to the size of the jump across element interfaces. Performing an error estimation is, hence, a trivial task for the DG method. After deciding whether to adapt an element, the next step is the decision between h- and p-adaptation. This requires the estimation of the local smoothness of the

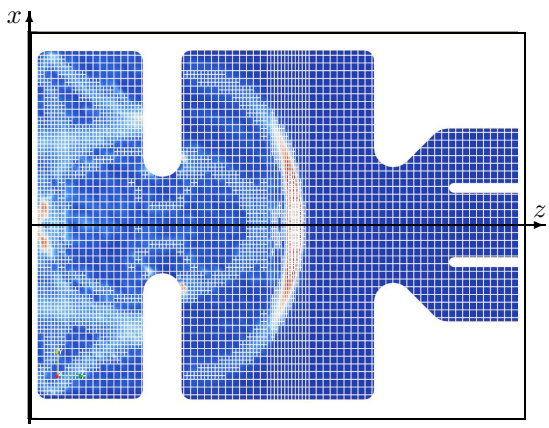

Figure 4: Snapshot of the total electric field excited by a bunch of particles in cut view. The upper half shows the electric field and the computational grid, the lower half shows the hp-adapted grid exclusively.

approximation. In [5, 10] smoothness indicators are presented.

We implemented an algorithm for performing automatic hp-adaptations for the scalar wave equation, which was tested on a Gaussian and trapezoidal wave packet as depicted in Fig. 5. There, the blue and green line represent the electric and magnetic field approximations. The gray dashed lines depict the position of the grid points and the height of the red circles indicate the approximation order employed for the respective element divided by ten. The snapshots were recorded after several hundreds of time steps. For the Gaussian packet the adaptation algorithm chooses medium sized to big elements and the preset maximum approximation order of five in the vicinity of the packet. For the non-smooth trapezoidal packet, the algorithm does not employ an approximation order above two throughout the simulation. In the vicinity of the pulse edges a high degree of h-refinement is applied, thus showing the desired behavior for the second packet as well.

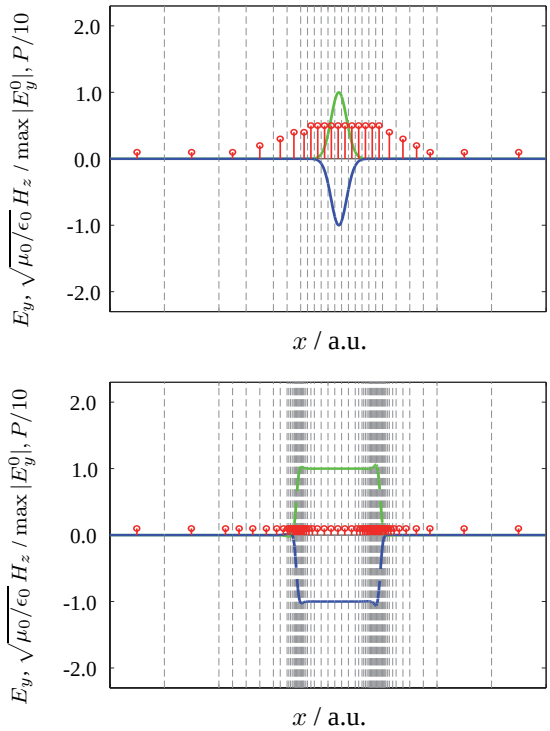

Figure 5: Simulation of a Gaussian and a trapezoidal wave packet using automated hp-adaptation. The electric field is plotted in blue and the magnetic field in green. The grid is indicated by gray dashed lines and the red circles indicate the approximation order used in the respective element.

CONCLUSIONS

Adaptation techniques for the high order DG method have been presented, which we apply on Cartesian grids using a tensor product basis of orthogonal basis functions. This particular setting allows us to perform h- and p-adaptations in a very efficient manner. Details of both kinds of adaptation were presented, and we showed that their application does not induce any instability. We performed hp-adaptive simulations and compared the results with the analytical solution. The hp-adaptive scheme was shown to require significantly less computational resources and time, yielding a higher accuracy as the non-adaptive method.

REFERENCES

[1] S. Schnepp, E. Gjonaj, and T. Weiland, “A Time-Adaptive Mesh Approach for the Self-Consistent Simulation of Particle Beams”, Int. Comp. Acc. Phys. Conf. (ICAP), 2006.

[2] E. Gjonaj, T. Lau, S. Schnepp, F. Wolfheimer, and T. Weiland, “Accurate Modelling of Charged Particle Beams in Linear Accelerators”, New Journal of Physics (8), 2006.

[3] E. Gjonaj, T. Lau, and T. Weiland, “Conservation Properties of the Discontinuous Galerkin Method for Maxwell Equations”, Int. Conf. Electromagnetics in Advanced Applications (ICEAA), 2007.

[4] J.S. Hesthaven, and G.B. Jacobs, “High-order nodal discontinuous Galerkin particle-in-cell method on unstructured grids”, J. of Comp. Phys. (214), 2005.

[5] S. Schnepp, “Space-Time Adaptive Methods for Beam Dynamics Simulations”, PhD thesis, TU Darmstadt, 2009.

[6] I.N. Onishchenko, D.Y. Sidorenko, and G.V. Sotnikov, “Structure of electromagnetic field excited by an electron bunch in a semi-infinite dielectric-filled waveguide”, Phys. Rev. E (65), 2006.

[7] A. Harten, “High Resolution Schemes for Hyperbolic Conservation Laws”, J. Comp. Phys. (49), 1983.

[8] K. Flöttmann, and F. Stephan, “BMBF Proposal for a RF Photoinjectors as Sources for Electron Bunches of Extremely Short Length and Small Emittance”, 1999.

[9] B. Cockburn, “Discontinuous Galerkin Methods”, Z. Angewandte Mathematische Mechanik (83), 2003.

[10] L. Krivodonova, N. Chevaugeon, and J. Flaherty, “Shock Detection and Limiting with Discontinuous Galerkin Methods for Hyperbolic Conservation Laws”, Appl. Numer. Math, 2004.